Navarro-Tapia, D., Marcos, A., Bennani, S., & Roux, C. (2016). Structured H-Infinity Control Based on Classical Control Parameters for the VEGA Launch Vehicle. In *2016 IEEE Conference on Control Applications (CCA 2016): Proceedings of a meeting held 19-22 September 2016, Buenos Aires, Argentina* (pp. 33-38). Buenos Aires, Argentina: Institute of Electrical and Electronics Engineers (IEEE). https://doi.org/10.1109/CCA.2016.7587818

Structured H-Infinity Control Based on Classical Control Parameters for the VEGA Launch Vehicle

Diego Navarro-Tapia[1], Andres Marcos[1], Samir Bennani[2] and Christophe Roux[3]

***Abstract*— This article describes a methodology for structured H-infinity synthesis that reconciles classical and robust control concepts. The aim is to provide a transparent and methodological process to tune the weights used in the structured synthesis. The process is exemplified on a simplified model for the atmospheric ascent-flight control system for the VEGA launch vehicle. The results show that the same gains used for a real flight can be recovered leading the path for industrial transfer of the H-infinity structured control to launchers.**

I. Introduction

The design of the ascent-flight control system of a launch vehicle for the atmospheric phase is still a challenging task. Along the first phase of the mission, any launch vehicle encounters undesired events such as wind disturbances, high aerodynamic pressure and dramatic dynamic changes.

The VEGA launcher [1] uses a classical controller framework for the Thrust Vector Control (TVC) system, which has been proved to be successful in the six flights VEGA has performed so far. Nonetheless, the need of providing higher robustness/performance as well as reducing the control tuning effort and cost prior each flight has lead to investigate the use of advanced and robust control techniques.

One of the most extended robust control techniques is H_∞, which has been successfully applied in a wide range of applications, see [2–5] for some aerospace operational examples. However, this theory has several limitations: firstly, the designed controller is usually of high-order and without a defined structured. This is an important drawback in aerospace applications where the computational power is limited. Besides, the lack of structure makes hard the understanding and tuning of the controller. Secondly, unlike classical control, H_∞ requirements are expressed in terms of weighting functions in the frequency domain. Thus, it is necessary a conversion between system requirements and H_∞ constraints.

In the last decade, two new approaches based on the H_∞ theory have been developed to solve some of the aforementioned problems. The *HIFOO* approach, which allows to synthesize controllers with a desired order [6], and the structured H_∞ approach (HINFSTRUCT), which allows to fix the order and structure of the controller [7].

[1] Diego Navarro-Tapia and Andres Marcos are with the Department of Aerospace Engineering, University of Bristol, BS8 1TR, United Kingdom diego.navarro-tapia/andres.marcos@bristol.ac.uk

[2] Samir Bennani is with ESA-ESTEC, Noordwijk, 2201AZ, The Netherlands samir.bennani@esa.int

[3] Christophe Roux is with ELV, Rome, 00034, Italy Christophe.Roux@elv.it

The structured H_∞ approach has been recently used in several investigations to design the control system for a launch vehicle [8–10]. However, this approach still requires advance knowledge and experience in expressing the system requirements in the frequency domain. In most of these works, this process is not explained in detail and since it generally implies several heuristic steps, it may be tedious to obtain an adequate set of weighting functions. These issues prevent the transfer of these control design methods to industry since the main requirements to accomplish this is the transparency and understanding of the process towards tuning, verification and validation.

In order to address the industrial needs and concerns, specifically for launchers but also in a more general manner for other types of systems, this paper extends the classical analysis done in [11], [12] and focuses on the selection of the weighting functions in terms of classical design parameters such as the natural frequency ω_n and the damping ratio ζ. Although the presented connections are well-known, a perusal of the state of the art seems to indicate that they have been forgotten (or rather, the design analysis has been shifted into a pure frequency-domain sensitivity functions perspective). It is within this aim of providing a more coherent and in-depth problem understanding, by connecting classical metrics and requirements with those from the sensitivity functions, that this work is presented. In addition, these connections provide a methodological framework for the weight selection that will facilitate the design task, as well as the subsequent controller tuning, verification and validation.

The layout of this paper is as follows. Firstly, the VEGA launcher and model are introduced in Section II. Secondly, the closed-loop, obtained using VEGA's controller architecture, is analysed connecting classical metrics and parameters with the H_∞ sensitivity functions framework. Then, the structured H_∞ approach is examined and the weighting functions are defined in terms of the launcher model parameters (a_6,k_1) and classical control requirements (ω_n,ζ). Finally, the process is exemplified using the rigid-motion of the VEGA launcher and the results discussed.

II. VEGA mission and launcher

VEGA launcher is the new European Small Launch Vehicle developed under the responsibility of the European Space Agency (ESA) and European Launch Vehicle (ELV) as prime contractor. The launcher has successfully performed six missions since February 2013.

The vehicle is assumed symmetric about the roll axis. Thus, considering the roll rate negligible, the cross coupling between the pitch and yaw axes are sufficiently small that can be ignored. This allows to simplify the design and analysis in a single plane, either the pitch or the yaw axis. In this work, the focus is on the yaw plane, see Figure 1.

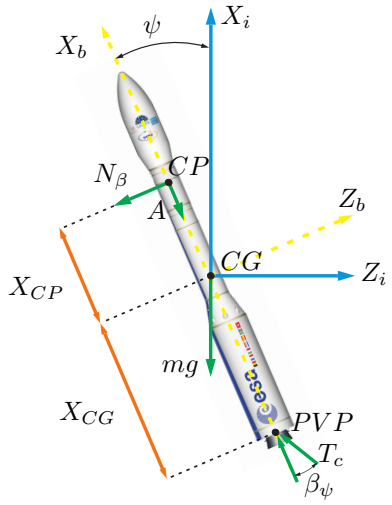

Fig. 1: VEGA yaw-motion diagram

The system used is based on a simplified rotational rigid motion model with the nozzle deflection angle β_ψ as the input and the yaw attitude angle ψ as the output (see equations 1 and 2).

$$\begin{bmatrix}\dot{\psi}\\ \ddot{\psi}\end{bmatrix} = \begin{bmatrix}0 & 1\\ a_6 & 0\end{bmatrix}\begin{bmatrix}\psi\\ \dot{\psi}\end{bmatrix} + \begin{bmatrix}0\\ k_1\end{bmatrix}\beta_\psi \tag{1}$$

$$\psi = \begin{bmatrix}1 & 0\end{bmatrix}\begin{bmatrix}\psi\\ \dot{\psi}\end{bmatrix} + \begin{bmatrix}0\end{bmatrix}\beta_\psi \tag{2}$$

Expressing the previous state-space representation as a transfer function, the plant model $G(s)$ is given by:

$$G(s) = \frac{\psi}{\beta_\psi} = \frac{k_1}{s^2 - a_6} \tag{3}$$

The previous model is simple yet significant. It contains the main launcher rigid motion effects, and can be easily augmented for design or analysis with additional effects (e.g. flexible, sloshing, actuator dynamics). Indeed, it is standard in industrial launcher design to start with this model [1], [13]. More fundamentally, it offers a simple launcher benchmark to demonstrate the connections between classical and modern control techniques.

Looking at equation 3, the plant model depends on two parameters: the aerodynamic instability coefficient a_6 and the controllability parameter k_1, whose expressions are given by:

$$a_6 = \frac{N}{J_{yy}} X_{CP} \tag{4}$$

$$k_1 = -\frac{T_c}{J_{yy}} X_{CG} \tag{5}$$

where, N is the total aerodynamic normal force, J_{yy} is the yaw moment of inertia, T_c is the gimballed control thrust force, X_{CP} is the distance from the center-of-pressure (CP) to the center-of-gravity (CG) and X_{CG} is the distance from CG to the nozzle pivot point (PVP). Note that the total aerodynamic force is given by: $N = QS_{ref}C_{N\beta}$ where Q is the dynamic pressure, S_{ref} is the reference area and $C_{N\beta}$ is the normal coefficient in the yaw plane.

a_6 and k_1 have a highly dynamic variation along the atmospheric phase trajectory as it can be seen in Figure 2, where these two parameters have been normalized by the maximum value of $|k_1|$. It should be remarked that k_1 has always a negative value (see equation 5). Also, the figure shows the ratio $a_6/|k_1|$, which is also an important parameter in the design trade-off process.

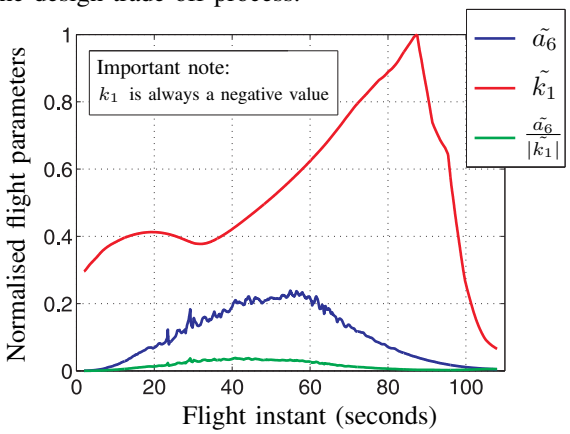

Fig. 2: Flight parameter evolution along the atmospheric phase

III. Classical control approach

The VEGA TVC control architecture [1] is based on a PD controller to stabilize the launcher's attitude, a lateral control feedback to reduce the angle of attack and to minimise the drift of the vehicle and a set of bending filters to attenuate the bending modes. A gain-scheduling approach is used for the PD and lateral controllers, using the time variation of a_6 and k_1 to focus on critical points along the flight trajectory (e.g. pitch-over, maximum dynamic pressure, maximum acceleration prior to stage separation). In this work we will only consider the rigid-motion PD controller.

First, the controller gains will be obtained and expressed in terms of an ideal 2^{nd} order response. Then, in order to provide insight on the weighting functions selection for the H_∞ synthesis, the closed-loop transfer functions are analysed in terms of the aforementioned parameters.

A. PD controller identification

Defining the controller as, $K(s) = K_p + K_d s$, and considering unity negative feedback, the closed-loop transfer function $T(s)$ from the reference input ψ_{ref} to the output ψ is:

$$T(s) = \frac{G(s)K(s)}{1 + G(s)K(s)} = \frac{k_1 K_d s + k_1 K_p}{s^2 + k_1 K_d s + k_1 K_p - a_6} \tag{6}$$

It is easy to recognize that the above can be represented as an ideal 2^{nd} order system with an extra zero z and gain A:

$$\frac{\psi}{\psi_{ref}} = \frac{{\omega_n}^2 A(s+z)}{s^2 + 2\zeta\omega_n s + {\omega_n}^2} = \frac{2\zeta\omega_n s + Az{\omega_n}^2}{s^2 + 2\zeta\omega_n s + {\omega_n}^2} \tag{7}$$

Equating equations 6 and 7, the controller gains can be expressed as a function of ω_n and ζ:

$$K_p = \left(1 + \frac{{\omega_n}^2}{a_6}\right)\frac{a_6}{k_1} \quad (8) \qquad K_d = \frac{2\zeta\omega_n}{k_1} \quad (9)$$

Also, in order to completely match equations 6 and 7, the steady-state value ψ_{ss} can be analytically represented as:

$$\psi_{ss} = Az = 1 + \frac{a_6}{{\omega_n}^2} \quad (10)$$

Since, at least for VEGA (but also usually for launchers in general), the control design objectives are defined in terms of margin requirements [1], the gain margin (GM) for rigid-motion is derived next following the same philosophy:

$$GM = 1 + \frac{{\omega_n}^2}{a_6} \quad (11)$$

It is important to remark now (see equations 10 and 11) that the ratio $a_6/{\omega_n}^2$ plays an important role for launchers since it can tune the tracking performance and the gain margin. Also, it is easy now to observe that when considering ω_n fixed, the most challenging design point occurs over the high dynamic pressure region where a_6 is at its maximum value (around the flight instant 55s in Figure 2). This leads to worst tracking performances and lower gain margins, and is in agreement with standard launcher knowledge and experience.

A similar phase margin (PM) definition was done but the resulting analytical expression is very involved, and in any case for the understanding and definition of PM requirements it is better to look at the sensitivity functions (see next subsections).

B. Sensitivity functions

A common way to study the robustness and performance of a system is to analyse the closed-loop transfer functions, also known as sensitivity functions.

1) Sensitivity function $S(s)$: represents the error between the reference input and the output. Note that the focus is on $S(s)$, as the complementary sensitivity function $T(s)$ is directly connected to it (see equation 12).

$$S(s) = 1 - T(s) = \frac{s^2 - a_6}{s^2 + 2\zeta\omega_n s + {\omega_n}^2} \quad (12)$$

In order to connect with the previous classical metrics, $|S(\omega)|$ can be derived from equation 12 as:

$$|S(\omega)| = \frac{\omega^2 + a_6}{\sqrt{\omega^4 + 2\omega^2{\omega_n}^2(2\zeta^2 - 1) + {\omega_n}^4}} \quad (13)$$

$|S(\omega)|$ has a high-pass filter shape, where the high-frequency gain equals 1 and the DC gain is given by:

$$|S(\omega = 0)| = \frac{a_6}{{\omega_n}^2} \quad (14)$$

Note that $a_6/{\omega_n}^2$ also appears here, reflecting the knowledge that the low frequency of S(s) serves to reflect tracking performance and gain margin.

Another relevant metric to study is the peak of the sensitivity function. Figure 3 shows the evolution of $|S(\omega_{peak})|$ in terms of $a_6/{\omega_n}^2$ and ζ variations.

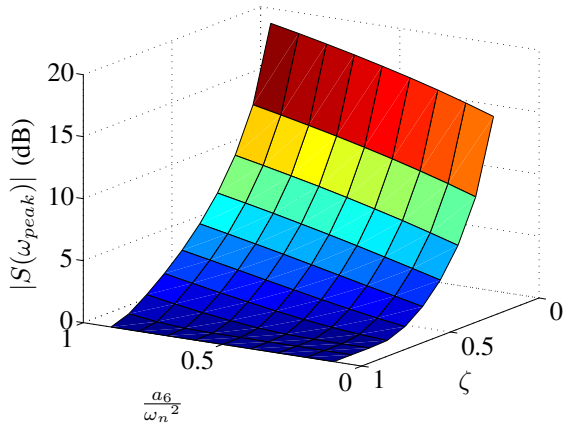

Fig. 3: $|S(\omega_{peak})|$ evolution in terms of $a_6/{\omega_n}^2$ and ζ

Notice from the figure that the maximum gain of $|S(\omega)|$ increases as ζ reduces. It is also seen that it increases with increasing $a_6/{\omega_n}^2$. Comparing this behaviour with equations 10 and 11, it can be concluded that lower peaks in $|S(\omega)|$ imply better tracking performances and better gain margins. This conclusion agrees with [14] where the following relation between the stability margins and $|S(\omega_{peak})|$ is shown:

$$GM \geq \frac{|S(\omega_{peak})|}{|S(\omega_{peak})| - 1} \quad (15) \qquad PM \geq 2\arcsin\left(\frac{1}{2|S(\omega_{peak})|}\right) \quad (16)$$

In preparation for the subsequent weight design, Figure 4 shows the evolution of $|S(\omega)|$ when independently varying each of the parameters ω_n, ζ and t. Firstly, see left plot, ω_n is varied from 1.7 to 2.3 rad/s with fixed $\zeta = 0.7$ and flight instant $t = 55s$. The plot shows that slower systems (i.e. low ω_n) present higher DC gains and maximum $|S(\omega)|$ values, which implies smaller stability margins and worst tracking performances in agreement with the analysis from equation 11.

Secondly, see the middle plot, the damping ratio ζ is varied from 0.1 to 1, under fixed $\omega_n = 1.5$ rad/s and $t = 55s$. $|S(\omega)|$ presents a higher peak as ζ is reduced, as expected from the correlation between damping and sensitivity peak.

Finally, the flight instant is varied from 10 to 110 seconds, for fixed $\omega_n = 1.5$ rad/s and $\zeta = 0.7$. As it was previously mentioned, when the time response parameters are fixed then $|S(\omega)|$ presents a higher peak as a_6 increases. In addition, it can be seen that tracking performance worsens around the high dynamic pressure region (i.e when a_6 is at its maximum value).

2) Control sensitivity function $KS(s)$: it represents the transfer function from the reference input ψ_{ref} to the control signal u generated by the controller, and is given by:

$$KS(s) = \frac{1}{k_1}\frac{(2\zeta\omega_n s + \psi_{ss}{\omega_n}^2)(s^2 - a_6)}{s^2 + 2\zeta\omega_n s + {\omega_n}^2} \quad (17)$$

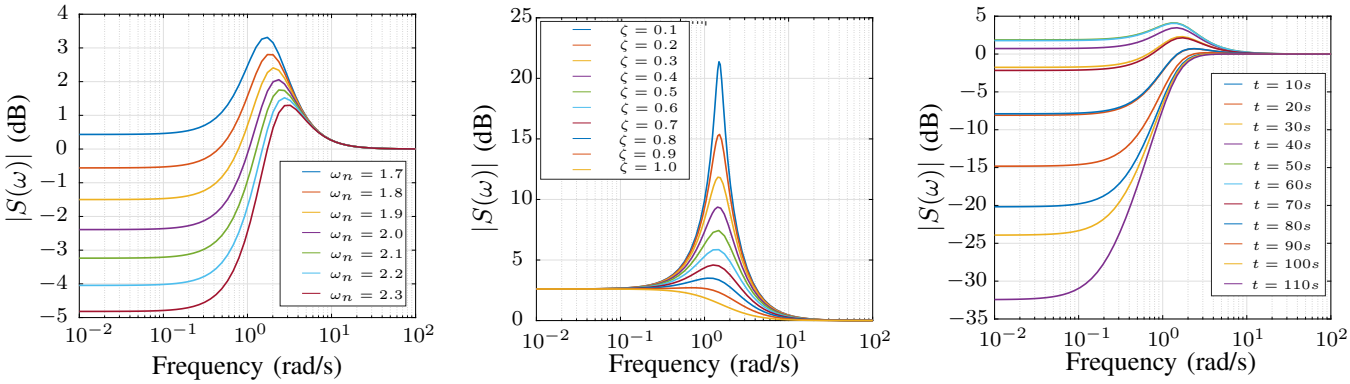

Fig. 4: $|S(\omega)|$ evolution based on changes for ω_n (left figure), ζ (middle figure) and flight instant (right figure).

$|KS(\omega)|$ has a high-pass filter shape, where the DC gain is given by equation 18. Similarly, it can be seen the dependency on the term ${a_6}/{\omega_n}^2$ and on this case also $a_6/|k_1|$ (whose variation along the atmospheric flight is depicted in Figure 2).

$$|KS(\omega = 0)| = KS(t = \infty) = \frac{a_6}{|k_1|}(1 + \frac{a_6}{{\omega_n}^2}) \qquad (18)$$

Although the frequency analysis is relevant, in this case the time-domain analysis offers a more intuitive way to analyze this transfer function. Applying the Laplace inverse transform to equation 17, the time-domain function $KS(t)$ can be obtained (not shown due to space limitations).

In order to analyze and establish requirements related to actuators' saturation is interesting to study the maximum value of $KS(t)$. Figure 5 shows the evolution of $KS(t_{peak})$ in terms of ${a_6}/{\omega_n}^2$ and ζ variations (for the flight instant $t = 55s$).

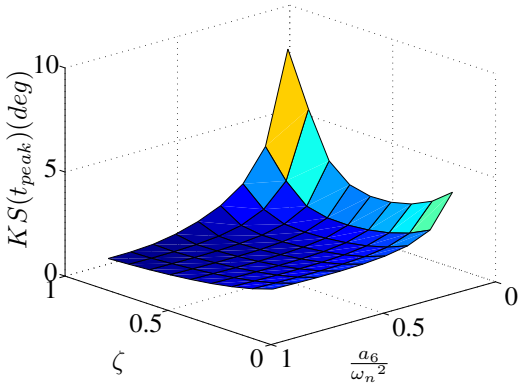

Fig. 5: $KS(t_{peak})$ evolution in terms of $\frac{a_6}{{\omega_n}^2}$ and ζ $(t = 55s)$

Notice from Fig 5 that the lower ${a_6}/{\omega_n}^2$ is, the higher the value of $KS(t_{peak})$ becomes. That means that higher gain margins and better tracking performances imply more actuator effort. This undesired effect can be alleviated by tuning the damping ratio ζ at the expense of increasing system overshoot.

From the previous analyses, it can be concluded that good tracking performance (i.e. low ${a_6}/{\omega_n}^2$) and plant input limitation to avoid actuator saturation (i.e. low initial and maximum values of $KS(t)$) are conflicting requirements. Nonetheless, this trade-off can be alleviated by tuning the damping ratio. Thus, based on the presented analyses a clear design trade-off to emerge (based on the ratio ${a_6}/{\omega_n}^2$ and ζ), reconciling classical understanding with robust concepts.

IV. Structured H_∞ Synthesis

In this section the *hinfstruct* synthesis is examined. Then, using the analyses from the previous section, the weighting functions are expressed in terms of the launch vehicle model parameters (a_6,k_1) and classic control parameters (ω_n,ζ). Finally, the weighting functions are validated through an example for the VEGA Launcher.

A. Structured H_∞

In this work, a H_∞ mixed-sensitivity S-KS is considered. Thus, two weighting functions $W_s(s)$ and $W_u(s)$ will be used to constraint the sensitivity function $S(s)$ and the control sensitivity function $KS(s)$ respectively (see Figure 6).

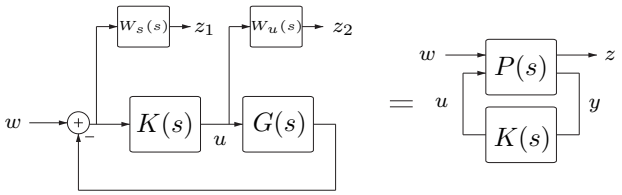

Fig. 6: Standard Form for Structured H_∞ Synthesis

This problem can be formulated using the Standard Form suggested in [7] (see Figure 6), where P is the Linear Fractional Transformation (LFT) model of the generalized plant (including the weighting functions), and $K(s)$ is the tunable structured controller: *K=ltiblock.pid('K','PD')*.

The classic H_∞ problem consists in minimizing the H_∞ norm of the transfer function from w to z (H_{zw}), which is given by the following lower LFT expression:

$$H_{zw} = P_{11} + P_{12}K(I - P_{22}K)^{-1}P_{21} = \begin{bmatrix} W_sS \\ W_uKS \end{bmatrix} \qquad (19)$$

However, as it is stated in [15], this configuration could provide misleading solutions when there are cross-couplings between the feedback loops. The structured H_∞ synthesis addresses this problem defining a generalized constraint H, which is the concatenation of all the H_∞ constraints in a diagonal block: $H = diag[W_s S, W_u K S]$.

B. Selection of the weighting functions

To facilitate tuning the weighting functions $W_s(s)$ and $W_u(s)$, a general format is used [14]. Specifically for $W_s(s)$:

$$W_s(s) = \frac{\frac{s}{h_s} + \omega_s}{s + \omega_s l_s} \tag{20}$$

where h_s and l_s are the high-frequency and low-frequency asymptotes of ${W_s}^{-1}(s)$ and ω_s is the crossover frequency.

For the sensitivity control function $KS(s)$, a constant weighting has been used to limit actuator magnitude:

$$W_u(s) = 1/A_u \tag{21}$$

Next, and based on the analyses from the previous section, the parameters of $W_s(s)$ and $W_u(s)$ are expressed as a function of the system response parameters (ω_n and ζ) and the launcher model parameters (a_6 and k_1):

$$l_s = \frac{a_6}{{\omega_n}^2} 10^{\frac{0.45}{20}} \tag{22}$$

$$h_s = \begin{cases} 10^{\frac{0.45}{20}} & \text{if } |S(\omega_{peak})| = 1 \\ 10^{\frac{H(a_6,\omega_n,\zeta)}{20}} & \text{other} \end{cases} \tag{23}$$

$$\omega_s = \Omega(a_6, \omega_n, \zeta) \tag{24}$$

$$A_u = \begin{cases} 10^{\frac{53}{20}} & \text{if } |S(\omega_{peak})| = 1 \\ |\frac{a_6}{k_1}| 10^{\frac{U(a_6,\omega_n,\zeta)}{20}} & \text{other} \end{cases} \tag{25}$$

The functions H, Ω and U have been defined based on an heuristic examination of a grid of points along the trajectory and a range of ω_n and ζ values. These functions are shown in Figure 7 and detailed next. It is noted that the definition of these functions is critical for the connection of the classical metrics and system analyses presented before (and favored by industry) with the definition of the frequency-domain weight requirements required by H_∞ techniques. Also, although the specific values are system dependent, the analysis and definition rationale presented in here are general.

a) Selection of l_s: the definition of equation 22 is driven by the DC gain of $|S(\omega)|$ from equation 14. A heuristic gap of 0.45dB has been added to allow free-play of the optimizer between achieving the desired DC gain and satisfying the required constraint given by the inverse of $W_s(s)$.

b) Selection of h_s: the proposed high-frequency asymptote is based on the maximum gain of $|S(\omega)|$. From the analysis presented in the previous section, $|S(\omega_{peak})|$ decreases as ζ increases and as ${a_6}/{\omega_n}^2$ decreases. This $|S(\omega_{peak})|$ evolution is used to define equation 23. As above, a gap over $|S(\omega_{peak})|$ at high frequencies is added. This gap is constant when $|S(\omega_{peak})| = 1$. Otherwise, h_s is a function of the damping ratio ζ and the term ${a_6}/{\omega_n}^2$ (see the left plot of Figure 7).

c) Selection of ω_s: the proposed ω_s is based on the crossover frequency of $|S(\omega)|$. It was seen before that the bandwidth increases as ζ increases and as ${a_6}/{\omega_n}^2$ decreases. Thus, equation 24 is defined capturing this behavior. When the maximum gain of $|S(\omega)|$ equals 1, ω_s is a function of the damping ratio ζ and the term ${a_6}/{\omega_n}^2$. Otherwise, the value of ω_s is maintained constant (see the middle plot of Figure 7).

d) Selection of A_u: as for the above, A_u is based on the analyses from the previous sections. When $|S(\omega_{peak})| = 1$, A_u has a constant value of 53 dB, which was obtained heuristically. Otherwise, A_u depends on two terms: $|\frac{a_6}{k_1}|$ (which models the dependency of $KS(s)$ on this term) and the function U (which models its evolution as ${a_6}/{\omega_n}^2$ and ζ vary).

It should be mentioned that the weighting functions defined in equations 20 and 21 are only valid for ζ values higher than 0.4. The reason is that a first order weighting function, such as that proposed for $W_s(s)$, cannot capture the high order response of $|S(\omega)|$ with low damping ratios (see the middle plot of Figure 4). In any case, this does not imply a limitation because responses with such low damping ratios are undesirable as they result in very high overshoots and very low stability margins.

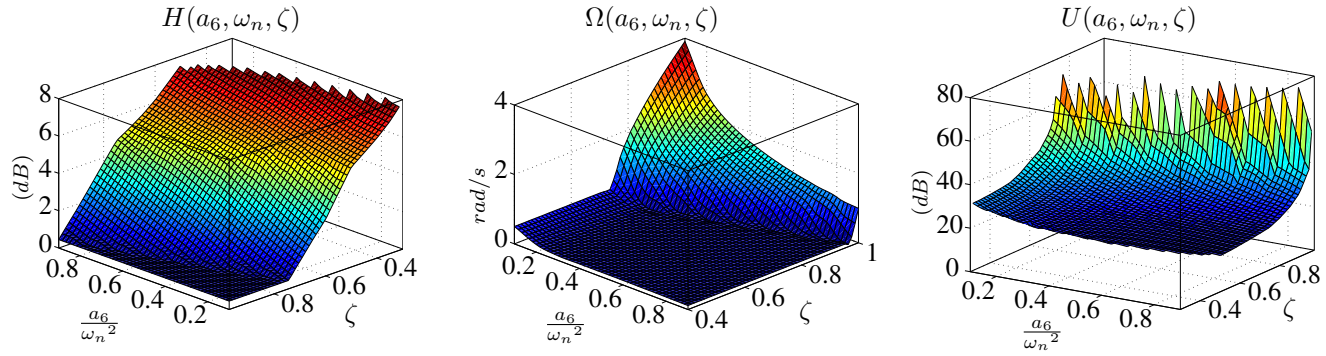

Fig. 7: Functions H, Ω and U

C. VEGA example

The weighting functions presented above are applied to a rigid-motion example for the VEGA launcher.

This example considers two Linear Time Invariant (LTI) models of the VEGA launcher at two flight instants: $t = 30s$ (Mach 1) and $t = 55s$ (maximum dynamic pressure). Table I shows the system parameters used in the third flight of VEGA. Note that these parameters have been normalized by the values for $t = 55s$ for confidentially reasons.

t	$a6/\tilde{\omega_n}^2$	$\tilde{\zeta}$	$a_6/\tilde{\lvert k_1 \rvert}$
30s	0.5113	0.6269	0.9006
55s	1	1	1

TABLE I: Normalized system parameters for VEGA

Using equations 22-25, two different set of weighting functions are obtained for each flight instant (see their inverses in Figure 8). Using these weighting functions, two PD H_∞ controllers are obtained. To validate the designs, Figure 8 compares the frequency responses using the two designed controllers and the baseline controllers (in black). Note that the baseline controller gains can be computed using equations 8-9. Although difficult to see in Figure 8, the frequency responses of the different controllers match respectively at each time instant. This implies that given the same conditions and design objectives, the same controllers that were used as baseline can be recovered from a structured H-infinity framework. This has the important implication that the legacy knowledge and experience (and even controller structure) can be used within a design framework that provides better robustness and performance guarantees, as well as more efficient tuning and V&V capabilities.

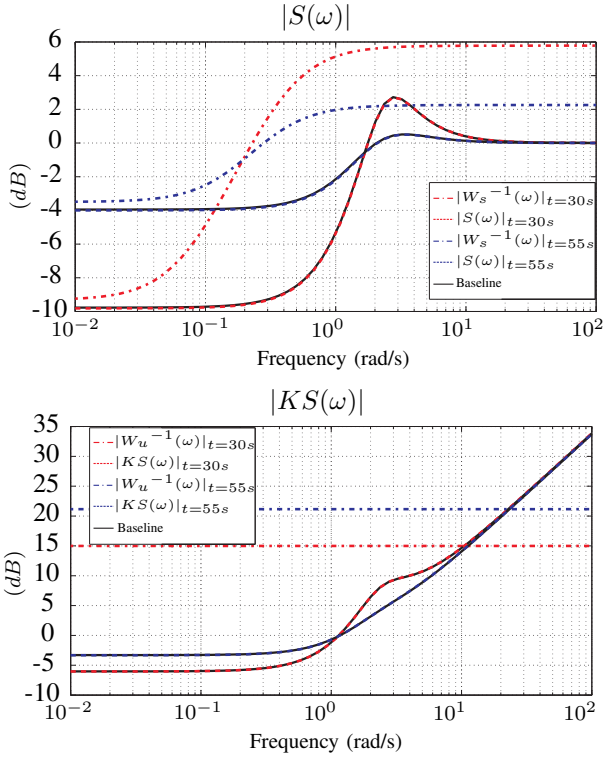

Fig. 8: $|S(\omega)|$ and $|KS(\omega)|$ [$t = 30s$ (red) and $t = 55s$ (blue)]

V. Conclusion

In this work, a methodological framework to select the weighting functions for structured H-infinity synthesis has been presented and applied to the design of the VEGA launch vehicle attitude control.

The process uses well-known correlations between classical and robust metrics, but with the goal of identifying critical parameters from these correlations. These identified parameters and trends facilitate in turn the design trade-off analyses and thus, naturally lead towards a methodological way to define the weights required for the subsequent H_∞ design. Specifically, the sensitivity functions have been analyzed in terms of the launch vehicle parameters and classical design parameters such as the natural frequency ω_n and the damping ratio ζ.

This methodology shown in this work allows the designer to facilitate the design task, as well as the subsequent tuning, verification and validation.

Acknowledgment

This work was jointly funded by ESA/ELV through the Networking/Partnering Initiative contract No. 4000114460/15/NL/MH/ats as well as by the Engineering and Physical Sciences Research Council (EPSRC).

References

[1] C. Roux and I. Cruciani, "Scheduling schems and control law robustness in atmospheric flight of vega." ESA GNC Conference, 2008.

[2] C. Charbonnel, "H_∞ controller design and μ-analysis: Powerful tools for flexible satellite attitude control," in *AIAA Guidance, Navigation, and Control Conference*, August 2010.

[3] C. Pittet and C. Fallet, "Gyroless attitude control of a flexible microsatellite."

[4] S. Mauffrey, F. Chabert, and M. Schoeller, "H_∞ control for ariane 5 plus launcher: the industrialisation of a new technology," in *Proceedings of the 5^{th} International Conference on Launcher Technology*, 2003.

[5] Y. Morita and J. Kawaguchi, "Attitude control design of the m–v rocket," *Philosophical Transactions of the Royal Society of London A: Mathematical, Physical and Engineering Sciences*, vol. 359, no. 1788, pp. 2287–2303, 2001.

[6] J. V. Burke, D. Henrion, A. S. Lewis, and M. L. Overton, "Hifoo - a matlab package for fixed-order controller design and H_∞ optimization," in *Proceedings of the IFAC Symposium on Robust Control Design*, 2006.

[7] P. Gahinet and P. Apkarian, "Structured H_∞ synthesis in matlab," in *Proceedings of the IFAC World Congress*, 2011, pp. 1435–1440.

[8] M. Knoblauch, D. Saussié, and C. Bérard, "Structured H_∞ control for a launch vehicle," in *American Control Conference*, 2012.

[9] D. Saussié, Q. Barbès, and C. Bérard, "Self-scheduled and structured H_∞ synthesis: a launch vehicle application," in *American Control Conference*, 2013, pp. 1590–1595.

[10] D. S. de la Llana, S. Bennani, I. Cruciani, and J. Aranda, "H-infinity control of the vega launch vehicle first stage in presence of roll," in *IFAC Symposium of Automatic Control in Aerospace*, 2013, pp. 54–59.

[11] E. Gadea, "Design of a robust controller for the vega tvc using the μ-synthesis technique," Master's thesis, ESA-ESTEC, 2011.

[12] M. A. de Virgilio and D. K. Kamimoto, "Practical applications of modern controls for booster autopilot design," in *Proceedings of the 12^{th} Digital Avionics Systems Conference*, 1993, pp. 400–412.

[13] A. G. Brito, W. C. L. Filho, and F. O. Ramos, "Approach comparison for controller design of a launcher," in *Proceedings of the 6^{th} International ESA Conference on GNC Systems*, 2005.

[14] S. Skogestad and I. Postlethwaite, *Multivariable feedback control: analysis and design*. John Wiley & Sons, 2005.

[15] P. Gahinet and P. Apkarian, "Descentralized and fixed-structure H_∞ control in matlab," in 50^{th} *IEEE Conference on Decision and Control and European Control Conference*, 2011, pp. 8205–8210.